Biophysical Journal
Article

Biophysical Society

Divide & Conquer: Surfactant Protein SP-C and Cholesterol Modulate Phase Segregation in Lung Surfactant

Nuria Roldan,[1,2] Jesús Pérez-Gil,[1,2] Michael R. Morrow,[3] and Begoña García-Álvarez[1,2,*]
[1]Department of Biochemistry, Faculty of Biology, Complutense University, Madrid, Spain; [2]Healthcare Research Institute of Hospital 12 de Octubre, Hospital Universitario 12 de Octubre, Madrid, Spain; and [3]Department of Physics and Physical Oceanography, Memorial University of Newfoundland, St. John's, Newfoundland, Canada

ABSTRACT Lung surfactant (LS) is an essential system supporting the respiratory function. Cholesterol can be deleterious for LS function, a condition that is reversed by the presence of the lipopeptide SP-C. In this work, the structure of LS-mimicking membranes has been analyzed under the combined effect of SP-C and cholesterol by deuterium NMR and phosphorus NMR and by electron spin resonance. Our results show that SP-C induces phase segregation at 37°C, resulting in an ordered phase with spectral features resembling an interdigitated state enriched in dipalmitoylphosphatidylcholine, a liquid-crystalline bilayer phase, and an extremely mobile phase consistent with small vesicles or micelles. In the presence of cholesterol, POPC and POPG motion seem to be more hindered by SP-C than dipalmitoylphosphatidylcholine. The use of deuterated cholesterol did not show signs of specific interactions that could be attributed to SP-C or to the other hydrophobic surfactant protein SP-B. Palmitoylation of SP-C had an indirect effect on the extent of protein-lipid perturbations by stabilizing SP-C structure, and seemed to be important to maximize differences among the lipids participating in each phase. These results shed some light on how SP-C-induced lipid perturbations can alter membrane structure to sustain LS functionality at the air-liquid interface.

INTRODUCTION

Lipid-protein interactions constitute the driving force for several processes that are essential for life. One vital example is breathing, supported by a lipid-protein complex lining the alveolar air-liquid interface. This complex, called lung surfactant (LS), is responsible for keeping lungs open during expiration. To do so, LS lowers surface tension to values close to 0 mN/m during exhalation, thus minimizing energy requirements for reopening the air-exposed surfaces of the lungs.

A specific protein and lipid composition sustains LS complex structure, characterized by bilayer and nonbilayer phospholipid-based organizations. In addition to dipalmitoylphosphatidylcholine (DPPC) (~40% LS total mass), lipids such as phosphatidylglycerol and cholesterol (~5–10%) confer to LS optimal properties to fulfill its surface-active function. Surfactant-associated proteins (SPs) represent less than 10% of LS dry weight, of which the small lipopeptide SP-C accounts for ~1% (1).

SP-C is the most abundant protein in LS in molar terms, and it has been considered as a specific marker of lung tissue (2,3). This transmembrane protein of 35 residues (4.2 kDa) is one of the most hydrophobic proteins known, and is present mainly as an α-helical peptide (4). This protein has also been suggested to oligomerize (5–7), a property that has been related to SP-C-induced membrane rearrangements (8,9). It has been noted that SP-C is involved in promoting lipid adsorption to the air-liquid interface (10,11), and it is reported to alter lipid organization in membranes (8,9,12,13). SP-C palmitoylation, in two adjacent cysteines at the N-terminal segment, is thought to promote monolayer-bilayer and bilayer-bilayer contacts, such as those potentially required for the generation of the so-called surfactant reservoir (14). This reservoir would supply surface-active material during inspiration (when the alveolar area is expanded), whereas during expiration, it would incorporate all those components squeezed out during compression of the surface film.

Cholesterol represents the major neutral lipid in surfactant, accounting for ~5–10% of LS whole mass. Whether cholesterol presence is beneficial or adverse for surfactant function is a controversial issue. Numerous studies support

Submitted January 9, 2017, and accepted for publication June 26, 2017.
*Correspondence: begoga01@ucm.es
Editor: Mei Hong.
http://dx.doi.org/10.1016/j.bpj.2017.06.059

the theory that cholesterol impairs proper surfactant function (15,16); however, others agree that a certain amount of cholesterol is needed for providing LS with optimal rheological properties and viscosity (17,18). Gómez-Gil et al. (15) reported that cholesterol impaired the biophysical function of an SP-B-containing surfactant preparation, but this impairment was reversed by the presence of the proper amount of SP-C. This affirmation was confirmed later by Baumgart et al. (16), who highlighted the importance of SP-C palmitoylation for restoring the function of a cholesterol-containing surfactant. We have previously demonstrated that SP-C alters cholesterol distribution in surfactant, generating highly curved structures that finally bud from the membrane (9). This evidence, connecting SP-C and cholesterol in surfactant, suggests that SP-C could have a role in limiting cholesterol levels at the interfacial film, supporting LS functionality at the air-liquid interface.

Deuterium NMR (^{2}H NMR), phosphorus NMR (^{31}P NMR), and electron spin resonance (ESR) are powerful tools to investigate lipid-protein interactions, such as those occurring in LS. Indeed, they have been used before to assess SP-C effect on membranes (12,19–22). However, little information is available about SP-C behavior in a lipid environment formed by mixtures of saturated and/or unsaturated phospholipids incorporating physiological amounts of cholesterol. For this reason, our work aimed to analyze the combined effect of SP-C and cholesterol on LS-mimicking membranes from a structural point of view, also taking into account the effect of SP-C palmitoylation.

Our results suggested that in the absence of cholesterol, SP-C is able to induce phase segregation, generating a highly immobilized lipid phase regardless of the palmitoylation state of the protein. This immobilizing effect could correlate with the induction of an interdigitated phase, an effect previously attributed to SP-C (22). This behavior was observed in all the phospholipids studied, but DPPC seemed to be the most affected one. These results were supported by ESR measurements, which also suggested an increase of average order in the membrane induced by the protein. ^{2}H NMR results indicated that cholesterol increases lipid order and reduces lipid mobility at 37°C. This effect was enhanced by the presence of SP-C. Although SP-C-induced phase segregation in the presence of cholesterol was not clear at 37°C, the combined effect of SP-C and cholesterol resulted in POPC-d_{31} phase separation at 30°C. Our results suggested that the SP-C-ordering effect follows different patterns depending on the presence of the sterol, and that it could be sensitive to cholesterol amount.

We concluded that SP-C is able to substantially increase membrane order in an LS-mimicking environment, and that this effect could be independent of its palmitoylation state. SP-C and cholesterol in combination resulted in strongly immobilized lipid systems that exhibited phase separation in response to changes in temperature.

MATERIALS AND METHODS

1,2-Dipalmitoyl-sn-glycero-3-phosphocholine (DPPC), 1-palmitoyl-2-oleoyl-sn-glycero-3-phosphocholine (POPC), 1-palmitoyl-2-oleoyl-sn-glycero-3[phospho-rac-(1-glycerol)] (POPG), and chain-perdeuterated DPPC-d_{62}, POPC-d_{31}, and POPG-d_{31} were purchased from Avanti Polar Lipids (Alabaster, AL) and used without further purification and characterization (Fig. S1 *a*). Cholesterol-2,2,3,4,4,6-d6 (Chol-d_6) was obtained from Cambridge Isotope Laboratories (Tewksbury, MA). Unlabeled cholesterol and Tris were obtained from Sigma-Aldrich (St. Louis, MO).

For ESR experiments, 1-palmitoyl-2-stearoyl-(n-doxyl)-sn-glycero-3-phosphocholine labeled in n5 (5-PCSL) or n12 (12-PCSL) was also purchased from Avanti Polar Lipids (Fig. S1 *b*).

High-performance liquid chromatography-grade chloroform (Chl) and methanol (MeOH) were obtained from LabScan (Gliwice, Poland).

Protein purification

Native SP-B and SP-C were isolated from porcine lungs as described (23), and the native hydrophobic protein fraction of surfactant, containing SP-B and SP-C in the natural proportion occurring in LS (~1:1), was obtained using established methods (24). Nonpalmitoylated human recombinant SP-C (rSP-C) was purified according to the method in Roldan et al. (25). The identity and purity of each protein was assessed by sodium dodecyl sulfate polyacrylamide gel electrophoresis (SDS-PAGE) and quantified by amino-acid analysis. The sequence and structure of both SP-C and rSP-C is shown in Fig. S2 *b*.

SDS-PAGE

To assess differences in protein aggregation state, we conducted an SDS-PAGE analysis employing a gradient precast gel (4–20% acrylamide) (Bio-Rad, Madrid, Spain). Protein bands were visualized by silver staining and quantified by densitometry. The percentage monomer was calculated as the percentage area in the monomer band (~4 kDa) relative to the total area corresponding to all protein configurations.

Sample preparation for NMR

To simulate the lipid composition of LS membranes, we used a lipid mixture containing DPPC/POPC/POPG (50:25:15 w/w/w), which resembles the physiological proportion of zwitterionic/anionic and saturated/unsaturated phospholipid species occurring naturally in most lung surfactants (26–29). For ^{2}H NMR experiments, the corresponding natural lipids were replaced by deuterated versions in the mixture, as indicated (Fig. S1 *a*). Lipid stocks were prepared in Chl/MeOH 2:1 v/v and assessed for phosphorus content before use (30). Lipid and lipid-protein samples were prepared by mixing individual components in Chl/MeOH 2:1 v/v and drying the mixture by rotary evaporation at 50°C. We used 12.6 mg of phospholipid per sample, and 5 wt% (1 mol%) protein and/or 10 wt% cholesterol was incorporated when indicated. Solvent traces were removed by vacuum for at least 6 h, and samples were kept at −20°C until used. Multilamellar suspensions were obtained by the addition of Tris buffer (5 mM Tris (pH 7), 150 mM NaCl) at 60°C and vortexing to yield a final phospholipid concentration of 45 mg/mL. For ^{31}P NMR experiments, samples were similarly mixed and dried. The reconstitution step was performed at 60°C using a ThermoMixer (Eppendorf, Hamburg, Germany) with intermittent shaking. Samples were carefully transferred to 8 or 5 mm NMR tubes for ^{2}H NMR and ^{31}P NMR respectively and sealed.

For samples containing Chol-d_6, the amount of material was increased to 25.5 mg of phospholipid, and proteins were included as follows: 5 wt% (1 mol%) SP-C or rSP-C, 5 wt% (0.5 mol%) SP-B, and 5 wt% (~0.6 mol%) SP-B/C. Samples were processed as previously mentioned, and hydrated in 350 μL of Tris buffer.

NMR spectra acquisition

^{31}P NMR spectra were collected in a Bruker AV 500 MHz (11.74 T) with a 5 mm BBO probe, and referenced to 85% phosphoric acid in deuterium oxide. ^{31}P NMR spectra were acquired with proton decoupling during signal acquisition, and 5120 scans were accumulated. A 5-s recycle delay between scans was used to minimize radio frequency sample heating. Temperature was calibrated using deuterated methanol as an NMR thermometer (31).

For ^{2}H NMR, samples were positioned in a cylindrical coil and the probe was placed into the NMR spectrometer. Samples were allowed to equilibrate to the desired temperature for at least 15 min before each measurement. Temperature was measured and controlled to $\pm 0.1^{\circ}$C using a digital temperature controller (model 325; Lakeshore Cryotronics, Westerville, OH). ^{2}H NMR spectra were collected in a 9.4 T superconducting solenoid operating at resonance frequency of 61.42 MHz for deuterium nuclei. A quadrupole echo sequence was used ($\pi/2-t-\pi/2-$acq), with $\pi/2$ pulses of 5–6 μs separated by 35 μs (32). Data were collected using a 1-μs digitizer dwell time, with 8192 points in each channel. Oversampling by a factor of 4 was applied to give an effective dwell time of 4 μs (33). The free-induction decay was left shifted to place the echo maximum at the first point. To obtain doublet splittings corresponding to a specific bilayer orientation, dePaking of ^{2}H NMR spectra was conducted using the approach suggested by McCabe and Wassall (34).

For each deuterium spectrum of samples containing DPPC-d_{62}, 40,000–48,000 transients were averaged. For samples containing POPC-d_{31}, 80,000 transients were averaged, and for POPG-d_{31}, 96,000 transients were averaged. In the case of samples with deuterated cholesterol, 176,000 transients were averaged.

Sample preparation for ESR

A total of 0.9 mg of lipid or lipid/protein samples were prepared by mixing individual components in Chl/MeOH 2:1 v/v. Then, 1 mol% of spin-labeled probe was added in organic solvent. Samples were dried under a constant stream of nitrogen, and solvent traces were vacuum-evaporated for 2 h using a SpeedVac Concentrator System (ThermoFisher Scientific, Waltham, MA). Until hydrated, samples were kept at -20°C. Hydration was performed at 55°C for 1 h by addition of Tris buffer to a final phospholipid concentration of 11.25 mg/mL in a ThermoMixer (Eppendorf), with intermittent shaking. Samples were transferred to 1-mm capillaries and spun down at 21,100 $\times$ g at 4°C using a Sorvall microfuge equipped with a capillaries rotor. Excess of supernatant was removed, and capillaries were flame-sealed before measurements.

ESR spectroscopy

ESR spectra were recorded in a Bruker EMX 10/12 spectrometer equipped with a nitrogen-flow temperature regulation system. Sample capillaries were inserted into a quartz tube, with silicone oil for thermal stability. Typically, two scans were accumulated to improve signal/noise ratio, with a 4-min scan time. Spectra were collected using the WinEPR software with the following instrumental settings: 10 mW microwave power, 1.25-G modulation amplitude, 100 kHz modulation frequency, 0.33 s time constant, 100-G scan range, and 3360-G center field.

Differential scanning calorimetry

Differential scanning calorimetry of the different lipid and lipid/protein systems was carried out in a VP-DSC differential scanning calorimetry (DSC; MicroCal, Northampton, MA). Two different membrane systems were analyzed in the presence or absence of 5 wt% SP-C (1 mol%) and/or 10 wt% cholesterol, at a final phospholipid concentration of 1–2 mM. Multilamellar suspensions of DPPC-d_{62}/POPC/POPG and DPPC/POPC-d_{31}/POPG were prepared as described for ^{31}P NMR experiments at 60°C. Samples and reference cells were heated from 15 to 60°C at 0.5°C/min, and 15 cycles were collected. Data were analyzed using ORIGIN software (MicroCal) after baseline correction and concentration normalization.

RESULTS

^{2}H-NMR spectroscopy

SP-C has been linked to cholesterol regulation in LS. In addition, protein palmitoylation has been postulated as an important factor for the maintenance of LS functionality in the presence of cholesterol. However, to date, every attempt to prove a direct SP-C/cholesterol interaction has failed. Therefore, the objective of this work was to obtain detailed information of the effect of SP-C, SP-C palmitoylation, and cholesterol on membrane structure and dynamics by means of ^{2}H NMR.

As an LS model system, membranes of DPPC/POPC/POPG (50:25:15 w/w/w) were employed. For ^{2}H NMR experiments, deuterated lipids (Fig. S1 *a*) were used to label three equivalent lipid systems: DPPC-d_{62}/POPC/POPG, DPPC/POPC-d_{31}/POPG, and DPPC/POPC/POPG-d_{31}. Comparing observations on these systems allowed us to analyze the behavior of each component independently, either in the pure lipid system or in the presence of SP-C or rSP-C and/or cholesterol.

Powder spectra obtained at 37°C from samples with different deuterated lipid components are shown in Fig. 1. Those corresponding to pure lipid systems in the absence of cholesterol (Fig. 1, *a*–c, *bottom spectra*) exhibit sharp Pake doublet features, with splittings of $\Delta\nu$, characteristic of perdeuterated acyl chains undergoing axially symmetric reorientation about randomly oriented lipid bilayer normals. These spectra are representative of multilamellar membrane suspensions in the liquid-crystalline phase. Each deuteron contributes a doublet with prominent edges arising from molecules reorienting about symmetry axes that are perpendicular to the applied magnetic field. The splitting of the prominent edges for a given deuteron is proportional to the orientational order parameter for that carbon-deuterium bond, $S_{CD} = \langle 3\cos^2\theta_{CD} - 1\rangle/2$, where θ_{CD} is the angle between the carbon-deuterium bond and the symmetry axis, and the average is over motions that modulate the orientation-dependent quadrupole interaction on the timescale of the NMR experiment. Thus, for a perdeuterated phospholipid chain, the resulting spectrum is a superposition of doublets reflecting the orientational order for every position along the chain. A less restricted, more isotropic reorientation correlates with smaller splittings, as occurs for those deuterons located at the highly mobile methyl end of the acyl chain. More restricted motions, such as those of acyl chain methylene groups closer to the phospholipid polar headgroup, result in larger quadrupole splittings. The prominent edges at about ± 15 kHz reflect the existence of a plateau in the

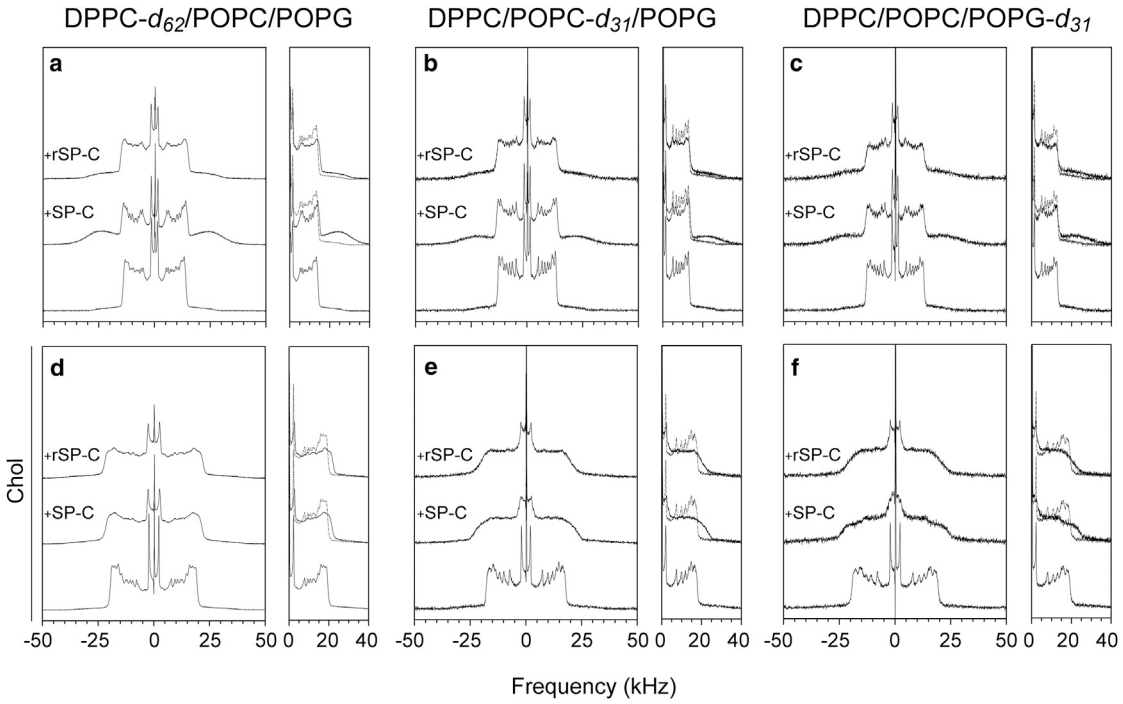

FIGURE 1 ^{2}H NMR powder spectra measured at 37°C for (*a* and *d*) DPPC-d_{62}/POPC/POPG, (*b* and *e*) DPPC/POPC-d_{31}/POPG, and (*c* and *f*) DPPC/POPC/POPG-d_{31}. (*d–f*) Samples incorporating 10 wt% cholesterol. Addition of 5 wt% (1 mol%) SP-C or 5 wt% (1 mol%) rSP-C results in an increase in orientational order for all the combinations tested. For simple visual comparisons, the right panel for each lipid combination represents the lipid-only spectrum (*bottom*), and an overlay of the lipid/SP-C (*middle*) and lipid/rSP-C (*top*) with the protein-containing spectra is represented as a solid line.

orientational order parameter profile of the saturated acyl chain on each deuterated lipid species (35).

For DPPC-d_{62}/POPC/POPG (Fig. 1 *a*), the addition of 5 wt% (1 mol%) SP-C resulted in a relative decrease in the intensity of the Pake doublet spectral components corresponding to liquid-crystalline phase bilayers, and in the appearance of broad spectral wings with peak intensities at $\sim\pm24$ kHz, and methyl group doublets (±7 kHz) with notably large splittings. This spectral line shape is characteristic of highly ordered lipid chains undergoing reorientation that is not axially symmetric over the NMR timescale ($\sim10^{-5}$ s). The superposition of spectral components corresponding to a liquid-crystalline phase and a highly ordered phase for this sample suggest an SP-C-induced phase separation. Spectra similar to the highly ordered phase component have been attributed to interdigitated lipid bilayers at high pressures (36–39), but the interpretation of the broad spectral component should be approached cautiously, since other bilayer phases can produce a comparably high orientational order. However, it must be noted that the ordered spectrum does not represent a typical gel phase, since intensity does not monotonically decrease with increased splitting. Incorporation of rSP-C also promoted the appearance of a component corresponding to highly ordered lipids in the spectra for all three deuterated lipids, but the fraction of each lipid in the highly ordered phase was smaller. However, a DPPC-d_{62}-labeled lipid preparation incorporating another stock of rSP-C showed a behavior similar to SP-C-containing samples (Fig. S2 *a*). SP-C palmitoylation stabilizes protein α-helical structure, preventing its aggregation (40); therefore, nonacylated SP-C versions are more prone to aggregate, and that can result in significant differences between stocks, in terms of protein structure. Such behavior was observed and described in Fig. S2, *c* and *d*. The observed difference between the effects of acylated and nonacylated SP-C (Fig. 1 *a*) could thus be an indirect consequence of protein acylation state. A nonacylated, partially aggregated stock would result in a less effective protein, given that aggregated rSP-C cannot incorporate into membranes. Thus, the absence of SP-C palmitoylation may not preclude the formation of a highly ordered phase, but might indirectly reduce the fraction of lipid that partitions into the highly ordered phase.

Quantification of the partitioning of deuterated lipid between different phases can be complicated by the possibility of differences in quadrupole echo decay time between the different phases. However, unnormalized versions of the lipid-only and lipid/SP-C spectra in Fig. 1 *a*, collected from samples containing nominally identical amounts of DPPC-d_{62} using the same number of scans, do integrate to areas that differ by only 4%. This suggests that quadrupole echo decay times for the two phases are similar, and thus spectral subtraction can provide an estimate of DPPC-d_{62} partitioning between the coexisting liquid crystal and highly

ordered phases observed in the lipid/SP-C sample. For the DPPC-d_{62} spectra in Fig. 1 *a*, it was found that subtracting 0.65 times the lipid-only spectrum from the lipid/SP-C spectrum eliminated most of the liquid-crystalline spectral intensity from the lipid/SP-C spectrum (Fig. S3 *a*). Although the difference spectrum still contained some sharp features due to slight differences in liquid-crystal phase splittings between the two phases, this result suggests that, in the lipid/SP-C sample, ~35% of the DPPC-d_{62} was in the highly ordered phase. Similar subtractions carried out for the lipid-only and lipid/SP-C spectra of Fig. 1, *b* and *c* suggest that 20–25% of the POPC-d_{31} and ~25–30% of the POPG-d_{31} in lipid/SP-C samples partition into the highly ordered phase (Fig. S3, *b* and *c*). These estimates indicate that, compared with the overall lipid composition of each sample, the SP-C-induced ordered phase is slightly enriched in DPPC-d_{62} and slightly depleted in POPC-d_{31}.

The observed partitioning of the three lipid components into the highly ordered phase suggests that the SP-C-induced ordered phase accommodates DPPC-d_{62} and POPG-d_{31} to a greater extent than POPC-d_{31}. The accommodation of DPPC-d_{62} may reflect an affinity of the saturated-chain phospholipid for the highly ordered environment of the SP-C-induced phase. Electrostatic interactions have been suggested between the positively charged SP-C and POPG in physiological-like conditions (22). In the ordered phase, the stronger accommodation of POPG-d_{31} relative to POPC-d_{31} may reflect a balance between an electrostatically favored compatibility with the SP-C-rich phase, and a reduced compatibility between unsaturated lipid chains and the highly SP-C-induced ordered environment due to mechanical mismatch. The partitioning of the three lipids into the small fraction of ordered phase induced by rSP-C was not as differentiated, suggesting that palmitoylation might amplify differences in the capacity of the SP-C-induced ordered phase to accommodate different lipids.

The comparisons illustrated in Fig. 1, *a–c* suggest that, at 37°C, the addition of SP-C to DPPC/POPC/POPG mixed-lipid bilayers induces separation into a highly ordered, possibly interdigitated phase that is enriched in SP-C and a liquid-crystalline phase. The latter appears to differ only slightly from the corresponding lipid-only DPPC/POPC/POPG phase in terms of average chain order and dynamics, as confirmed by the dePaked spectra (Fig. S4) and order parameter profile (Fig. S5). This analysis also shows that SP-C affects DPPC dynamics to a greater extent than POPC or POPG, which remain unaltered in the fluid phase upon protein incorporation (Fig. S5).

The spectra in Fig. 1, *d–f* show that, when cholesterol is incorporated into the lipid phase, the effect of SP-C on the mixture is different. Addition of 10 wt% cholesterol to the DPPC/POPC/POPG lipid mixtures resulted in an increase in quadrupole splittings for deuterons on each of the deuterated lipids (Fig. 1, *d–f*, *bottom spectra*). Such cholesterol-induced ordering of lipid acyl chains is typical of the liquid-ordered phase observed in a number of lipid-cholesterol mixtures (41–43).

In contrast to the absence of cholesterol, where SP-C induces the separation of a highly ordered phase from a largely unperturbed lipid phase at 37°C, the effects of adding SP-C to the cholesterol-containing lipid mixtures appear to be more subtle, possibly because of the high degree of orientational order already imposed by the presence of cholesterol.

The middle spectra of Fig. 1, *d–f* show how the combination of cholesterol and SP-C affect the ^{2}H NMR spectra for each of the lipid components in the mixture. The DPPC-d_{62} spectrum for lipid/cholesterol/SP-C (Fig. 1 *d*, *middle spectrum*) still displays a clear vertical edge, corresponding to the orientational order parameter plateau, at $\sim \pm 20$ kHz. This suggests that the DPPC-d_{62} acyl chain reorientation in the mixture with cholesterol and SP-C is still axially symmetric. Pake doublets corresponding to individual methylene deuterons, however, are less sharply resolved in this spectrum. This broadening suggests that the correlation time for reorientation is larger than in the absence of SP-C, and is approaching the upper threshold for fast motions on the ^{2}H NMR timescale. In the spectra for POPC-d_{31} and POPG-d_{31} in the corresponding mixtures (Fig. 1, *e* and *f*, *middle spectra*), methylene doublets are unresolved.

The loss of resolution in the POPC-d_{31} and POPG-d_{31} spectra for the lipid/cholesterol/SP-C mixtures could reflect acyl chain reorientation that is too slow to be axially symmetric on the ^{2}H NMR timescale, or it could reflect intermediate rate exchange between domains, for which acyl chain order differs slightly (42). In the POPG-d_{31} spectrum for this mixture (Fig. 1 *f*, *middle spectrum*), there is a small spectral edge with a splitting similar to the plateau splitting in the corresponding lipid-only spectrum (Fig. 1 *e*, *bottom spectrum*) and evidence of a narrower methyl doublet. At 30°C, the POPC-d_{31} spectrum for the lipid/cholesterol/SP-C mixture is a superposition of two components and indicates separation into a more ordered and liquid-crystalline phase (Fig. S3, *b* and *c*). For the corresponding mixture containing DPPC-d_{62}, however, the spectrum at 30°C (Fig. S3 *a*) shows no evidence of phase separation, and is characteristic of reorientation that is not axially symmetric on the ^{2}H NMR timescale.

The spectra shown in Fig. 1, *d–f* suggest that in DPPC/POPC/POPG (50:25:15 w/w/w) mixtures containing 10 wt% cholesterol, the addition of 5 wt% (1 mol%) SP-C affects the dynamics of all three lipid components, but not necessarily in the same ways. To gain more insight into the dynamics of bilayer components in the lipid/cholesterol/SP-C bilayers, ^{2}H NMR spectra were obtained from a series of bilayer mixtures containing Chol-d_6. Fig. 2 *a* shows the structure of cholesterol, including the deuteron locations. The bottom spectrum of Fig. 2 *b* is obtained from DPPC/POPC/POPG (50:25:15 w/w/w) containing 10 wt%

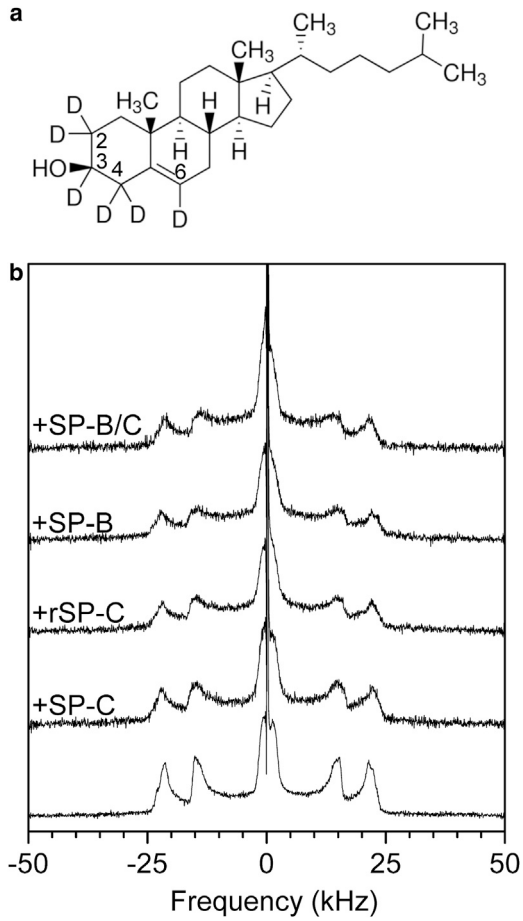

FIGURE 2 (*a*) Structure of Chol-d_6. Deuterated positions are numbered. (*b*) Powder spectra of DPPC/POPC/POPG (50:25:15, w/w/w) +10 wt% Chol-d_6 measured at 37°C. The effects of the different proteins incorporated (SP-C, rSP-C, SP-B, or SP-B/C) on the spectrum were not substantially different.

Chol-d_6 at 37°C. In comparison with previously reported spectra for Chol-d_6 in DMPC membranes (44), the doublet with the largest splitting can be assigned to the deuteron on carbon 3 and to the axial deuterons on carbons 2 and 4. The doublet with a splitting of $\sim\pm 15$ kHz can be assigned to the equatorial deuterons on carbons 2 and 4. The central doublet with a very small splitting can be assigned to the deuteron on carbon 6.

The addition of SP-C has little effect on the doublet splittings, but does result in some broadening of the line shape and an overall reduction in area of the unnormalized spectrum by about half. This appears as a decrease in the signal/noise ratio of the normalized spectra shown in Fig. 2. Addition of rSP-C, SP-B, or the hydrophobic protein fraction of native LS, SP-B/SP-C, has a similar effect on the Chol-d_6 spectrum. Comparison of the lipid/Chol-d_6 and lipid/Chol-d_6/protein spectra indicates that the orientational order of the rigid portion of Chol-d_6 is not affected by the addition of SP-C or any of the proteins. The insensitivity of the observed splittings to the addition of SP-C suggests that the observed line broadening and loss of intensity cannot be due to intermediate rate exchange between environments in which the deuterons have different splittings.

The SP-C-induced line broadening in the Chol-d_6 spectrum appears to reflect a change in reorientational correlation time, rather than intermediate rate exchange between domains with differing degrees of orientational order. If the line broadening observed for DPPC-d_{62}, POPC-d_{31}, and POPG-d_{31} in the lipid/cholesterol/SP-C mixtures is also due to SP-C-induced changes in reorientational dynamics, then the difference in the degree of line broadening for POPC-d_{31} and POPG-d_{31}, compared with DPPC-d_{62} in the 37°C spectra shown in Fig. 1, *d–f* is interesting. It suggests that in the relatively ordered environment of the lipid/cholesterol bilayer, the reorientations of POPC and POPG are relatively more hindered than the reorientation of DPPC. This may reflect a greater capacity of the saturated lipid to accommodate to the joint ordering influence of cholesterol and SP-C compared with that of the two monounsaturated lipids. It should be noted, however, that chain perdeuteration reduces the gel-to-liquid crystal transition temperature of DPPC-d_6 by 3–4°C (45). Perdeuteration of the saturated chains in POPC-d_{31} and POPG-d_{31} also lower their main transition temperatures, but these are presumably below the 37°C temperature at which the spectra in Fig. 1 were obtained.

To assess the extent to which relative deuteration levels might contribute to observed differences in line broadening for the lipid/SP-C/cholesterol spectra of Fig. 1, *d–f*, DSC thermograms were obtained for DPPC-d_{62}- and POPC-d_{31}-containing systems. As suggested above, the melting temperatures for the lipid-only and lipid/cholesterol mixtures differed by ~4°C, depending on which lipid was deuterated (Fig. S7). Conversely, the incorporation of SP-C resulted in similar melting temperatures for both lipid mixtures, regardless of whether or not cholesterol was present. The initial transitions for the lipid/SP-C/cholesterol mixtures were slightly below 30°C, and thus well below 37°C, suggesting that the difference in line broadening observed for the differently labeled mixtures at 37°C was due to a difference in lipid environment rather than a shift in the transition temperature of the mixture. Interestingly, the proximity of the lipid/SP-C/cholesterol transition to 30°C may account for the evidence of phase coexistence in the lipid/SP-C/cholesterol spectra observed at 30°C in the mixtures containing POPC-d_{31} or POPG-d_{31}, but not for the mixture containing DPPC-d_{62}.

As noted in Fig. S7, the transition observed for the SP-C-containing liposomes continued to increase with each DSC cycle (up to at least 15 cycles). This may reflect a tendency for the protein to promote membrane rearrangements that could cause lipid demixing, or it could reflect a compositional refinement of membranes resulting from SP-C-induced membrane fragmentation (9,13). This remains a question for future study.

^{31}P NMR

To further investigate SP-C-induced effects on lipid configuration at the headgroup level, membranes of DPPC/POPC/POPG containing either SP-C or rSP-C were analyzed by ^{31}P NMR. Fig. 3 illustrates the ^{31}P NMR spectra obtained for nonoriented vesicles of lipid alone, or those containing SP-C or rSP-C at 37°C. Liposomes in the lamellar liquid-crystalline phase exhibit an axially symmetric chemical shift anisotropy (CSA) characteristic of the fast axial reorientation of lipid molecules, in which the line shape depends on ^{31}P headgroup orientation and disorder (46). In the absence of the protein, ^{31}P NMR spectra resulted in two differentiated peaks reflecting the different CSAs for POPG and POPC/DPPC, whose CSAs are very similar and cannot be distinguished in the powder pattern as it has been noted for clinical LS preparations (47–49). The spectral line shape for the lipid-only vesicles was characteristic of a lamellar liquid-crystalline phase (46). The addition of SP-C promoted a significant change of the spectral line shape. Spectral components corresponding to the lamellar liquid-crystalline phase were still present, but the two powder patterns became broadened in the presence of either SP-C or rSP-C, which could presumably indicate motions that are less axially symmetric, resulting from SP-C-induced ordering.

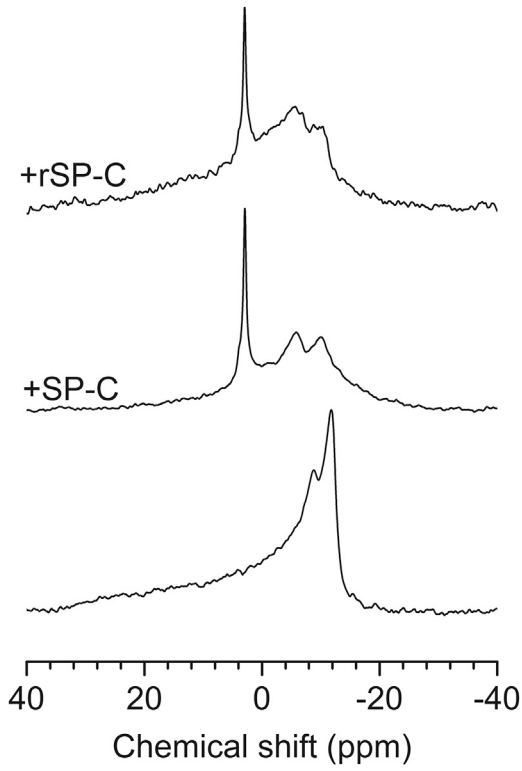

FIGURE 3 Powder ^{31}P NMR spectra of DPPC/POPC/POPG liposomes in the absence or presence of 5 wt% (1 mol%) SP-C (*middle spectrum*) or rSP-C (*top spectrum*).

Addition of the protein also resulted in the appearance of a sharp peak at ~3 ppm, which is presumably indicative of extensive SP-C-induced lipid reorganizations. These were apparently similar when either palmitoylated or nonpalmitoylated SP-C were present. This peak represented approximately ~15–20% of the total spectrum area, suggesting that a small proportion of lipids experienced an increase in motion at the headgroup level indicative of a substantial bilayer disruption. The appearance of such a narrow line shape is related with a rapid averaging on the NMR timescale, which has been previously associated with micelles in solution, or highly curved structures such as small unilamellar vesicles (50–54).

The absence of any spectral component at ~30–35 ppm (5–9) for the protein-containing liposomes rules out any significant preferential orientation of the bilayer normal along the magnetic field under the conditions used in this study.

ESR spectroscopy

To confirm our results on this SP-C-induced increase in lipid order, we performed ESR experiments using the same lipid system previously mentioned. Spin-labeled lipids can be incorporated into lipid bilayers in a low proportion without perturbing membrane behavior. In addition, different positions along the acyl chain and the phospholipid headgroup can be labeled, and it is possible to obtain information on the dynamics and conformational order of lipids at different levels within the membrane. Measurements were carried out at different temperatures and two different amounts of SP-C were tested: 5 wt% (1 mol%) and 10 wt% (2 mol%).

Two spin-probes, 12-PCSL and 5-PCSL, were incorporated in multilamellar vesicles of DPPC/POPC/POPG 50:25:15 (w/w/w). Results for 12-PCSL-containing samples are shown in Fig. 4. 12-PCSL is labeled in the n12 position, and therefore represents acyl chain mobility close to the hydrophobic core of the membrane. The increase in temperature resulted in line narrowing correlating with an increase in membrane fluidity. Samples incorporating SP-C showed broader spectra when compared with the lipid-alone sample, especially above 25°C. Greater differences were observed in the range from 30 to 37°C, where the pure lipid exhibited a spectrum characteristic of a more fluid character than the SP-C-associated ones. The two amounts of SP-C tested generated very similar spectra, although 10 wt% (2 mol%) protein restricted lipid motion to a slightly higher extent. This is reflected in an increased outer hyperfine splitting, $2A_{max}$, which is significantly higher for samples incorporating SP-C (Fig. 5). However, even though SP-C induces restriction in lipid motion as observed for the bulk fluid phase, we cannot distinguish a second immobilized component, which is in agreement with what was previously reported for this protein (12). These results are consistent with our previously observed, SP-C-induced immobilizing effect in the lipid system, and could support the

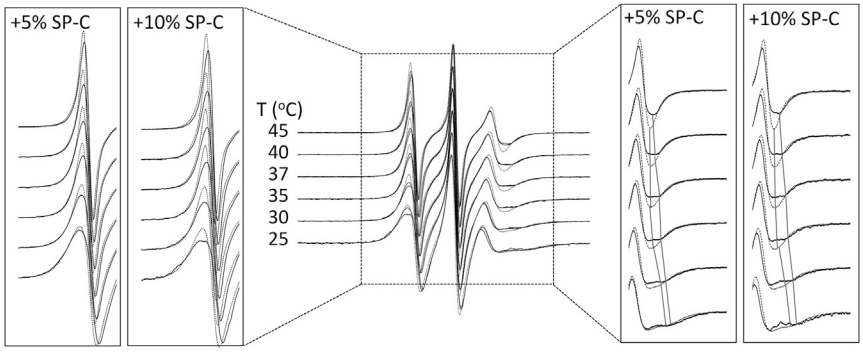

FIGURE 4 ESR spectra of DPPC/POPC/POPG membranes incorporating no protein (*dotted line*), 5 wt% (1 mol%) (*gray line*), or 10 wt% SP-C (2 mol%) (*black line*) labeled with 1 mol% of the probe 12-PCSL at different temperatures. The spectra on the left and right sides correspond to magnifications showing a detailed view of the low- and high-field spectra for membranes containing no protein (*dotted line*), and samples containing either 5 wt% (1 mol%) SP-C or 10 wt% SP-C (2 mol%) (*solid lines*). In the right panels, lines connecting consequent minimums have been added as a visual guide. The total scan range was 100 G.

interdigitated structure proposed. The induction of such a structure would require that all positions along the acyl chain showed a restricted motion under the presence of SP-C. Our results for samples incorporating a probe positioned closer to the lipid headgroup, 5-PCSL, suggest that SP-C also induced a trend toward higher splittings at this level (Fig. S8). Taken together, these results support the SP-C-induced restriction in the average lipid motion of the lipid system studied that could be mediated by the generation of an interdigitated structure.

DISCUSSION

The role of SP-C in LS membranes has been extensively analyzed. However, protein availability and instability, among other factors, have limited the elucidation of its mechanism of action. The particular lipid environment has been shown to modulate SP-C configuration in membranes (25), and therefore, careful selection of membrane composition is key to understanding SP-C function.

SP-C induces phase segregation

We assessed LS-mimicking membranes comprising the most representative lipid components of surfactant, DPPC/POPC/POPG (50:25:15 w/w/w). According to our results, SP-C is able to induce lateral phase segregation in the absence of cholesterol in that lipid environment. Such phase segregation occurred at near-physiological conditions (37°C (pH 7)) and resulted in a highly ordered lipid fraction involving the three phospholipids analyzed here. These results agree with existing literature, in which the generation of lipid nanodomains (55) or even immobilized lipid phases (22) have been observed upon addition of SP-C or SP-C N-terminal peptides, stressing SP-C capacity to alter lipid packing.

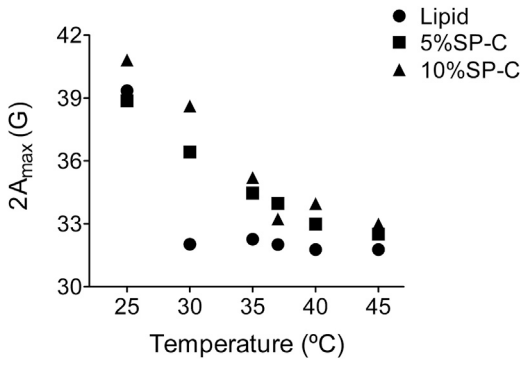

FIGURE 5 Outer hyperfine splittings ($2A_{max}$) of 12-PCSL-labeled samples containing no protein (*full circles*), 5 wt% (1 mol%) SP-C (*squares*), or 10 wt% (2 mol%) SP-C (*triangles*) as a function of temperature.

The liquid-crystalline phase observed in lipid/SP-C spectra (Fig. 1, *a–c*, *middle*) remained essentially unaltered compared with the lipid-only system, as observed in the order parameter profiles and dePaked spectra obtained from ^{2}H NMR (Figs. S4 and S5), suggesting either that SP-C is concentrated in the ordered regions or that its presence in the fluid regions causes no effect. The establishment of protein-protein interactions, already suggested in the literature (5–7), could promote a local concentration of SP-C. In addition, SP-C dimers could be the first stage in more extensive oligomerization, a possibility that has been already proposed as the cause of SP-C-induced packing defects or pores in membranes (8,9,13). This would be consistent with the behavior observed in this study, where the differential accommodation of lipids in the ordered structures induced by SP-C presence might be explained by selective protein-lipid interactions. We propose a model in which an increased protein density in localized regions of the membrane could amplify the extent of those interactions, triggering the lateral segregation suggested by our results (Fig. 6). This is supported by previous evidence showing SP-C confined localization, either at the boundaries of ordered/disordered domains in bilayers or condensed/expanded regions in monolayers (55–57). However, it must be noted that SP-C partitioning among domains cannot be directly deduced from the results shown in this study.

In the absence of cholesterol, the SP-C-induced ordered phase exhibited spectral features consistent with interdigitated structures (36–38). Nevertheless, as discussed previously, we cannot discard other lipid organizations that

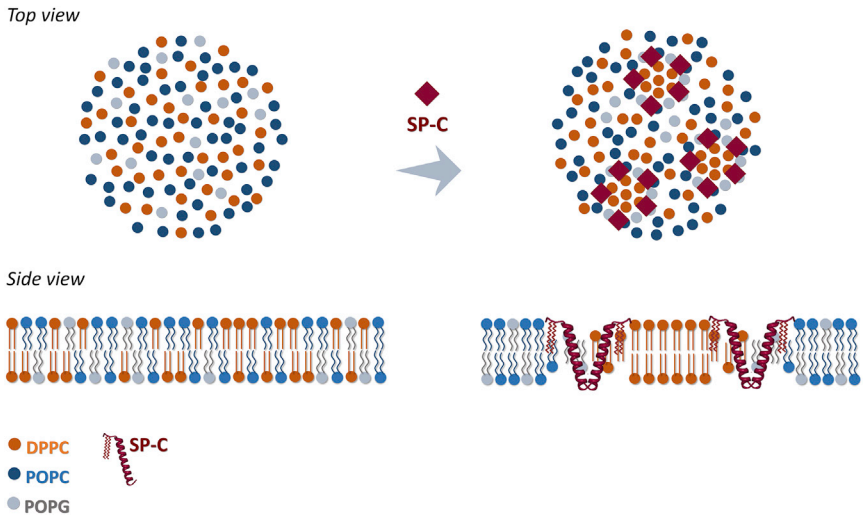

FIGURE 6 Model of the potential mechanism of SP-C-induced, selective lipid interdigitation. To see this figure in color, go online.

could result in spectra of similar characteristics. The effect of SP-C does not seem to be restricted to the acyl chains. ^{31}P NMR experiments confirmed the extensive membrane alterations induced by the protein, which resulted in the generation of a very dynamic phase and a phase with spectral features consistent with slightly constrained phosphates. The latter could represent the average behavior of those lipids involved in the ordered, interdigitated phase and those forming part of the liquid-crystalline phase as detected by ^{2}H NMR. However, the highly dynamic phase, which would appear as a central spike in our ^{2}H NMR spectra, is consistent with spectral shapes corresponding to micelles or small unilamellar vesicles (50–54), such as those already reported for SP-C (9).

ESR experiments showed a decrease in lipid mobility in the presence of SP-C, at levels close to the phospholipid headgroup (5-PCSL, Fig. S8), but also at the hydrophobic core of the membrane (12-PCSL, Fig. 4). This is consistent with the concept of an SP-C-induced ordering effect that could be related to an interdigitated phase, an effect that had been attributed specifically to the SP-C N-terminal segment (22). As was observed previously (12), ESR spectra do not show any features characteristic of a strongly immobilized lipid phase. This can be likely attributed to the particular properties of SP-C (4). The inability of spin probes to sense phase segregation in surfactant membranes has been described before (58) for studies in which ESR experiments were unable to detect phase separation observable by other techniques. This is likely explained by the structural complexity of surfactant assemblies and the intrinsically dynamic character introduced by the surfactant proteins SP-B and SP-C. Additionally, it must be considered that upon phase separation, spin probes can partition unevenly among domains providing only partial information in the system. The probes used in our approach were phosphatidylcholine-based nitroxide-labeled molecules and consequently, their behavior and partitioning might be more similar to that of POPC, a lipid that despite being more ordered upon SP-C presence, seems to be the least SP-C-influenced, according to ^{2}H NMR results.

In DPPC/POPC/POPG membranes, the SP-C-induced ordered phase was slightly enriched in DPPC and depleted in POPC. POPG, however, showed a behavior in between DPPC and POPC. This might be explained by a preference of DPPC for the SP-C-induced ordered environment, whereas POPG could prevail in the ordered phase over POPC due to electrostatic protein-lipid interactions. In line with ^{2}H NMR results, SP-C creates packing defects that can contribute to the observed phase segregation (59). That might facilitate adoption by the membrane of a certain curvature degree and fold, and the sorting out of unsaturated phospholipids from DPPC-enriched regions, as proposed in the model in Fig. 6. Given that DPPC can be packed more tightly than unsaturated lipids, this could be relevant for reaching low surface tensions during exhalation. The change in curvature could also explain, to some extent, SP-C-mediated lipid adsorption, which has been suggested to occur through a negatively curved stalk in cooperation with SP-B (60–62). For such a structure to occur, SP-B and SP-C would need to generate membrane curvature, a condition that although already demonstrated (9,63,64), does not provide enough mechanistic insights to determine how this process is accomplished. Thus, a possible implication of the potential SP-C-induced interdigitated phase might be the promotion of curved structures, the interdigitated phase being a possible intermediate state between the interfacial monolayer and the underlying bilayered reservoir. This would facilitate both adsorption and respreading of LS material, a function already related to SP-C-induced interdigitation (22). Indeed, lipid interdigitation combines a high degree of tail ordering and a high level of hydration of the headgroups, providing membrane characteristics that are intermediate between liquid-crystalline and gel phases. Shifting that to the LS context, a potential

SP-C-induced membrane interdigitation could also generate highly condensed lipid patches to provide stability to the multilayered interfacial film.

A mechanism for SP-C-induced interdigitation

The molecular basis behind a possible SP-C-induced interdigitation is an intriguing matter. SP-C is reported to cause changes in polarity in the membrane (12,19), an effect that is attributed to the N-terminal segment of the protein (19). ^{2}H NMR experiments revealed that SP-C perturbs the polar region of DPPC membranes, altering the disposition of the phosphate moiety in the membrane, in what has been proposed as a pulling effect toward the aqueous medium (19), and the ^{31}P NMR results shown in this study have also revealed great perturbing effects of SP-C at the phosphate region regardless of protein palmitoylation. Moreover, SP-C is reported to possess an intrinsic oligomerizing capacity (5–7); this, together with its tilted configuration in membranes (25), would extensively perturb lipid packing in the surrounding regions to which it is inserted. The combination of SP-C-induced lipid perturbations and the pulling effect could be interpreted as a first step toward protein-promoted interdigitation, so that SP-C could nucleate packing defects that could be relieved upon the adoption of a new lipid configuration.

The effect of SP-C palmitoylation

In this study, we also aimed to clarify the role of SP-C palmitoylation in the protein-induced membrane perturbations. The N-terminal segment of SP-C binds and disturbs phospholipid packing independently of its acylation (65,66), but N-terminal palmitoylation seemed to be determinant for promoting the membrane-ordering effect interpreted as interdigitation (22). Although our results suggest that palmitoylation seemed to enhance the extent of lipid perturbations, nonpalmitoylated SP-C showed a somewhat heterogeneous behavior depending on protein batches, some of them equaling the effects of the palmitoylated protein (Fig. S2 *a*). This highlights the importance of protein acylation in stabilizing protein structure and accordingly, protein functionality. Therefore, our results suggest that protein acylation has a rather indirect role on protein-induced effects. Given this evidence, the possibility that SP-C palmitoylation is not required for promoting membrane ordering cannot be ruled out. In contrast to the studies employing SP-C N-terminal peptides, full-length SP-C anchors the N-terminal segment to the membrane through the transmembrane α-helix. Therefore, acylation of the full-length protein might not be so critical compared with its importance for N-terminal peptides, a fact already suggested by Baumgart et al. (55), who showed no differences between SP-C and nonpalmitoylated recombinant versions in promoting membrane rearrangements. This is also consistent with the ^{31}P NMR results shown in this study, in which no significant differences were observed between SP-C- and rSP-C-containing samples. However, SP-C palmitoylation seemed to be important to magnify the differences between the lipids involved in SP-C-induced phase separation, suggesting that a nonpalmitoylated protein could be less effective in properly sorting out lipids.

Cholesterol/SP-C relationship

Cholesterol/SP-C relationship in surfactant has attracted an increasing amount of attention recently (9,15,16,67), but no clear connection between them has been established so far. In this regard, one of the objectives of this work was to elucidate the nature of the combined effect of SP-C and cholesterol on membranes mimicking LS composition. In DPPC/POPC/POPG membranes, cholesterol increased lipid order, as has been described for many other lipid-cholesterol combinations. However, the presence of SP-C resulted in a subtler effect when compared with the cholesterol-free system, where there was a marked phase separation into a highly immobilized phase and a liquid-crystalline phase. For lipid/cholesterol/SP-C samples, all phospholipids seemed to be more immobilized than in lipid/cholesterol membranes, displaying slower reorientations, especially in the case of POPC and POPG (Fig. 1, *e* and *f*). Their broadened POPC-d_{31} and POPG-d_{31} spectra indicated reorientations that were too slow to be axially symmetric on the ^{2}H NMR timescale, or possibly even an intermediate rate exchange between domains with slightly different chain order (42). DSC observations indicated that the mixtures were in similar states at 37°C regardless of which lipid was deuterated, leading to the conclusion that the observed differences in lipid dynamic must reflect differences in their environments.

Cholesterol deuteron quadrupole splittings were not substantially changed by the addition of protein (Fig. 2). For a rigid and planar structure such as cholesterol, only motions involving the whole molecule with respect to the bilayer normal could alter its order parameter, and consequently, its splittings. Different proteins were tested in an attempt to detect a specific protein/cholesterol interaction. Cholesterol deuteron splittings did not change substantially in the presence of SP-C, rSP-C, or SP-B, or when the native hydrophobic protein fraction of surfactant (SP-B/SP-C) was included; according to these results, specific perturbations on cholesterol behavior were not detected and could be discarded. Cholesterol remained oriented along the bilayer normal in all samples. However, the presence of the proteins slightly slowed cholesterol reorientation about its molecular axis, likely resulting from the overall increase in lipid order. It must be also noted that the central spike on the spectra could also be related with the generation of small vesicles induced by SP-C including cholesterol (9), which could also be relevant to explaining how SP-C could contribute to the compositional refinement of surfactant.

Although there was no evidence for phase segregation at 37°C for any of the preparations tested, DPPC/POPC-d_{31}/POPG did exhibit phase separation at 30°C only when SP-C and cholesterol were combined (Fig. S6, *b* and *c*). DPPC-d_{62}/POPC/POPG, however, did not show any signs of phase separations under those conditions (Fig. S6 *a*). The proximity of the transition to 30°C, as observed by DSC, may account for this difference. Interestingly, the addition of SP-C led to an increase in melting temperature with successive heating cycles. This effect could be related to membrane alterations resulting in lipid demixing or compositional refinement, which could be a consequence of the membrane-fragmenting behavior of SP-C (9,13) also suggested by our ^{31}P NMR results. Taken together, these observations indicate that the effects of SP-C and cholesterol on membrane architecture are subtly related and respond to changes in temperature in a coordinated manner, a fact than can be related to the response of surfactant to environmental changes as occurs for heterothermic animals (68). We speculate that differences in the responses of the saturated and unsaturated lipids to the presence of SP-C and cholesterol might be consistent with SP-C promoting a compositional refinement in the LS system, the ultimate purpose of which would be to maintain LS homeostasis and functionality, limiting cholesterol levels and unsaturated phospholipids at the functional interfacial film.

SP-C effect depends on lipid composition

These results show some discrepancies with similar studies assessing SP-C effects on lipid assemblies. Even though recent spectroscopic studies of LS have considered the complexity of surfactant composition (47–49), SP-C effects have been classically approached by using LS-mimicking systems including mainly saturated phospholipids (19–22), given that DPPC is the major lipid accounting for LS whole mass. In the majority of those lipid systems, little effect of SP-C was observed. A slight ordering on lipid acyl chains was generally attributed to its transmembrane character, but no noticeable lipid-immobilizing effect was detected, an effect related to this protein's small size and particular properties (4,12). However, under certain circumstances, even in those kinds of environments SP-C was proven to increase lipid order substantially. SP-C effect in DPPC membranes revealed the appearance of striated domains associated with a highly ordered lipid state (69), and in DPPC/dipalmitoylphosphatidylglycerol membranes, a palmitoylated N-terminal SP-C peptide was shown to be effective in promoting the formation of a highly immobilized lipid phase (22). In these studies, effects associated with hydrophobic mismatch or SP-C/lipid electrostatic interactions had to be taken into account, stressing the importance of providing a native-like lipid environment for SP-C to fulfill membrane rearrangements. We consider that the lipid system used in the current study provides an additional level of membrane complexity compared with previous works and at the same time, it more closely resembles the native protein environment.

CONCLUSIONS

Considering the results obtained in this study, SP-C restricts lipid mobility as previously reported (12,58), both in the absence and in the presence of cholesterol. SP-C is able to induce a highly ordered, possibly interdigitated phase. This provides some insights into how SP-C-induced membrane rearrangements could participate in processes such as lipid adsorption or DPPC enrichment at the interfacial film.

The combination of SP-C and cholesterol results in an increase in lipid chain order compared with cholesterol alone. SP-C/cholesterol samples behaved differently than those containing no cholesterol, suggesting that although SP-C induces an ordering effect in both cases, it also depends on the presence of the sterol. Such an effect could be potentially related to LS compositional refinement in membranes and films, relevant to maintaining LS homeostasis and functionality.

Understanding the molecular mechanisms supporting the combined effects of SP-C and cholesterol to alter membrane structure plays a crucial part in unraveling the physiological role of the SP-C/cholesterol relationship in the context of LS.

SUPPORTING MATERIAL

Eight figures are available at http://www.biophysj.org/biophysj/supplemental/S0006-3495(17)30743-9.

AUTHOR CONTRIBUTIONS

N.R. designed and performed the research, and analyzed and discussed the data. M.R.M. designed and supervised the research, contributed tools, and analyzed and discussed the data. J.P.-G. and B.G.-A. contributed tools, designed and supervised the research, and discussed the data. All authors wrote the manuscript and approved its final version.

ACKNOWLEDGMENTS

The authors are indebted to Dr. Valerie Booth, from Memorial University of Newfoundland, for providing laboratory facilities and fruitful discussions, and to Donna Jackman for assistance in sample preparation. The authors also acknowledge Dr. Antonio Cruz and Jose Carlos Castillo for their help in sample preparation for the ESR measurements, and their insightful suggestions and discussions. The authors also thank the Research Support Center for Resonance at the Complutense University, Madrid, Spain.

This work has been supported by grants from the Spanish Ministry of Economy (BIO2015-67930-R) and the Regional Government of Madrid (S2013/MIT-2807), and by a Natural Sciences and Engineering Research Council of Canada discovery grant to M.R.M. B.G.-A. is a recipient of a Ramon & Cajal contract. N.R. is a recipient of a Formación de Profesorado Universitario fellowship from the Spanish Ministry of Education, Culture and Sport.

SUPPORTING CITATIONS

References (70,71) appear in the Supporting Material

REFERENCES

1. Lopez-Rodriguez, E., and J. Pérez-Gil. 2014. Structure-function relationships in pulmonary surfactant membranes: from biophysics to therapy. *Biochim. Biophys. Acta.* 1838:1568–1585.
2. Korfhagen, T. R., S. W. Glasser, …, J. A. Whitsett. 1990. Cis-acting sequences from a human surfactant protein gene confer pulmonary-specific gene expression in transgenic mice. *Proc. Natl. Acad. Sci. USA.* 87:6122–6126.
3. Glasser, S. W., M. S. Burhans, …, T. R. Korfhagen. 2000. Human SP-C gene sequences that confer lung epithelium-specific expression in transgenic mice. *Am. J. Physiol. Lung Cell. Mol. Physiol.* 278:L933–L945.
4. Johansson, J., T. Szyperski, …, K. Wüthrich. 1994. The NMR structure of the pulmonary surfactant-associated polypeptide SP-C in an apolar solvent contains a valyl-rich alpha-helix. *Biochemistry.* 33:6015–6023.
5. Creuwels, L. A., R. A. Demel, …, H. P. Haagsman. 1995. Characterization of a dimeric canine form of surfactant protein C (SP-C). *Biochim. Biophys. Acta.* 1254:326–332.
6. Kairys, V., M. K. Gilson, and B. Luy. 2004. Structural model for an AxxxG-mediated dimer of surfactant-associated protein C. *Eur. J. Biochem.* 271:2086–2092.
7. Luy, B., A. Diener, …, C. Griesinger. 2004. Structure and potential C-terminal dimerization of a recombinant mutant of surfactant-associated protein C in chloroform/methanol. *Eur. J. Biochem.* 271:2076–2085.
8. Parra, E., A. Alcaraz, …, J. Pérez-Gil. 2013. Hydrophobic pulmonary surfactant proteins SP-B and SP-C induce pore formation in planar lipid membranes: evidence for proteolipid pores. *Biophys. J.* 104:146–155.
9. Roldan, N., T. K. M. Nyholm, …, B. García-Álvarez. 2016. Effect of lung surfactant protein SP-C and SP-C-promoted membrane fragmentation on cholesterol dynamics. *Biophys. J.* 111:1703–1713.
10. Oosterlaken-Dijksterhuis, M. A., H. P. Haagsman, …, R. A. Demel. 1991. Characterization of lipid insertion into monomolecular layers mediated by lung surfactant proteins SP-B and SP-C. *Biochemistry.* 30:10965–10971.
11. Wang, Z., O. Gurel, …, R. H. Notter. 1996. Acylation of pulmonary surfactant protein-C is required for its optimal surface active interactions with phospholipids. *J. Biol. Chem.* 271:19104–19109.
12. Pérez-Gil, J., C. Casals, and D. Marsh. 1995. Interactions of hydrophobic lung surfactant proteins SP-B and SP-C with dipalmitoylphosphatidylcholine and dipalmitoylphosphatidylglycerol bilayers studied by electron spin resonance spectroscopy. *Biochemistry.* 34:3964–3971.
13. Parra, E., L. H. Moleiro, …, J. Pérez-Gil. 2011. A combined action of pulmonary surfactant proteins SP-B and SP-C modulates permeability and dynamics of phospholipid membranes. *Biochem. J.* 438:555–564.
14. Na Nakorn, P., M. C. Meyer, …, H. J. Galla. 2007. Surfactant protein C and lung function: new insights into the role of alpha-helical length and palmitoylation. *Eur. Biophys. J.* 36:477–489.
15. Gómez-Gil, L., D. Schürch, …, J. Pérez-Gil. 2009. Pulmonary surfactant protein SP-C counteracts the deleterious effects of cholesterol on the activity of surfactant films under physiologically relevant compression-expansion dynamics. *Biophys. J.* 97:2736–2745.
16. Baumgart, F., O. L. Ospina, …, J. Pérez-Gil. 2010. Palmitoylation of pulmonary surfactant protein SP-C is critical for its functional cooperation with SP-B to sustain compression/expansion dynamics in cholesterol-containing surfactant films. *Biophys. J.* 99:3234–3243.
17. Leonenko, Z., S. Gill, …, M. Amrein. 2007. An elevated level of cholesterol impairs self-assembly of pulmonary surfactant into a functional film. *Biophys. J.* 93:674–683.
18. Kim, K., S. Q. Choi, …, J. A. Zasadzinski. 2013. Effect of cholesterol nanodomains on monolayer morphology and dynamics. *Proc. Natl. Acad. Sci. USA.* 110:E3054–E3060.
19. Morrow, M. R., S. Taneva, …, K. M. W. Keough. 1993. 2H NMR studies of the effect of pulmonary surfactant SP-C on the 1,2-dipalmitoyl-sn-glycero-3-phosphocholine headgroup: a model for transbilayer peptides in surfactant and biological membranes. *Biochemistry.* 32:11338–11344.
20. Dico, A. S., S. Taneva, …, K. M. W. Keough. 1997. Effect of calcium on phospholipid interaction with pulmonary surfactant protein C. *Biophys. J.* 73:2595–2602.
21. Simatos, G. A., K. B. Forward, …, K. M. Keough. 1990. Interaction between perdeuterated dimyristoylphosphatidylcholine and low molecular weight pulmonary surfactant protein SP-C. *Biochemistry.* 29:5807–5814.
22. Plasencia, I., F. Baumgart, …, J. Pérez-Gil. 2008. Effect of acylation on the interaction of the N-terminal segment of pulmonary surfactant protein SP-C with phospholipid membranes. *Biochim. Biophys. Acta.* 1778:1274–1282.
23. Pérez-Gil, J., A. Cruz, and C. Casals. 1993. Solubility of hydrophobic surfactant proteins in organic solvent/water mixtures. Structural studies on SP-B and SP-C in aqueous organic solvents and lipids. *Biochim. Biophys. Acta.* 1168:261–270.
24. Bernardino de la Serna, J., J. Perez-Gil, …, L. A. Bagatolli. 2004. Cholesterol rules: direct observation of the coexistence of two fluid phases in native pulmonary surfactant membranes at physiological temperatures. *J. Biol. Chem.* 279:40715–40722.
25. Roldan, N., E. Goormaghtigh, …, B. Garcia-Alvarez. 2015. Palmitoylation as a key factor to modulate SP-C-lipid interactions in lung surfactant membrane multilayers. *Biochim. Biophys. Acta.* 1848:184–191.
26. Baxter, C. F., G. Rouser, and G. Simon. 1969. Variations among vertebrates of lung phospholipid case composition. *Lipids.* 4:243–244.
27. Pfleger, R. C., R. F. Henderson, and J. Waide. 1972. Phosphatidyl glycerol–a major component of pulmonary surfactant. *Chem. Phys. Lipids.* 9:51–68.
28. Benson, B. J., J. A. Kitterman, …, W. H. Tooley. 1983. Changes in phospholipid composition of lung surfactant during development in the fetal lamb. *Biochim. Biophys. Acta.* 753:83–88.
29. Kahn, M. C., G. J. Anderson, …, S. B. Hall. 1995. Phosphatidylcholine molecular species of calf lung surfactant. *Am. J. Physiol.* 269:L567–L573.
30. Rouser, G., A. N. Siakotos, and S. Fleischer. 1966. Quantitative analysis of phospholipids by thin-layer chromatography and phosphorus analysis of spots. *Lipids.* 1:85–86.
31. Findeisen, M., T. Brand, and S. Berger. 2007. A 1H-NMR thermometer suitable for cryoprobes. *Magn. Reson. Chem.* 45:175–178.
32. Davis, J. H., K. R. Jeffrey, …, T. P. Higgs. 1976. Quadrupolar echo deuteron magnetic resonance spectroscopy in ordered hydrocarbon chains. *Chem. Phys. Lett.* 42:390–394.
33. Prosser, R. S., J. H. Davis, …, M. A. Lindorfer. 1991. 2H nuclear magnetic resonance of the gramicidin A backbone in a phospholipid bilayer. *Biochemistry.* 30:4687–4696.
34. McCabe, M. A., and S. R. Wassall. 1997. Rapid deconvolution of NMR powder spectra by weighted fast Fourier transformation. *Solid State Nucl. Magn. Reson.* 10:53–61.
35. Lafleur, M., B. Fine, …, M. Bloom. 1989. Smoothed orientational order profile of lipid bilayers by 2H-nuclear magnetic resonance. *Biophys. J.* 56:1037–1041.
36. Knight, C., A. Rahmani, and M. R. Morrow. 2016. Effect of an anionic lipid on the barotropic behavior of a ternary bicellar mixture. *Langmuir.* 32:10259–10267.
37. Singh, H., J. Emberley, and M. R. Morrow. 2008. Pressure induces interdigitation differently in DPPC and DPPG. *Eur. Biophys. J.* 37:783–792.

38. Rahmani, A., C. Knight, and M. R. Morrow. 2013. Response to hydrostatic pressure of bicellar dispersions containing an anionic lipid: pressure-induced interdigitation. *Langmuir.* 29:13481–13490.

39. Peng, X., A. Jonas, and J. Jonas. 1995. High pressure 2H-NMR study of the order and dynamics of selectively deuterated dipalmitoyl phosphatidylcholine in multilamellar aqueous dispersions. *Biophys. J.* 68: 1137–1144.

40. Gustafsson, M., W. J. Griffiths, …, J. Johansson. 2001. The palmitoyl groups of lung surfactant protein C reduce unfolding into a fibrillogenic intermediate. *J. Mol. Biol.* 310:937–950.

41. Linseisen, F. M., J. L. Thewalt, …, T. M. Bayerl. 1993. 2H-NMR and DSC study of SEPC-cholesterol mixtures. *Chem. Phys. Lipids.* 65:141–149.

42. Veatch, S. L., I. V. Polozov, …, S. L. Keller. 2004. Liquid domains in vesicles investigated by NMR and fluorescence microscopy. *Biophys. J.* 86:2910–2922.

43. Davis, J. H., J. J. Clair, and J. Juhasz. 2009. Phase equilibria in DOPC/DPPC-d62/cholesterol mixtures. *Biophys. J.* 96:521–539.

44. Dufourc, E. J., E. J. Parish, …, I. C. P. Smith. 1984. Structural and dynamical details of cholesterol-lipid interaction as revealed by deuterium NMR. *Biochemistry.* 23:6062–6071.

45. Guard-Friar, D., C. H. Chen, and A. S. Engle. 1985. Deuterium isotope effect on the stability of molecules: phospholipids. *J. Phys. Chem.* 89:1810–1813.

46. Seelig, J. 1978. 31P nuclear magnetic resonance and the head group structure of phospholipids in membranes. *Biochim. Biophys. Acta.* 515:105–140.

47. Antharam, V. C., R. S. Farver, A. Kuznetsova, K.H., …, J. R. Long. 2008. Interactions of the C-terminus of lung surfactant protein B with lipid bilayers are modulated by acyl chain saturation. *Biochim. Biophys. Acta.* 1778:2544–2554.

48. Antharam, V. C., D. W. Elliott, …, J. R. Long. 2009. Penetration depth of surfactant peptide KL4 into membranes is determined by fatty acid saturation. *Biophys. J.* 96:4085–4098.

49. Farver, S., A. N. Smith, …, J. R. Long. 2015. Delineation of the dynamic properties of individual lipid species in native and synthetic pulmonary surfactants. *Biochim. Biophys. Acta.* 1848:203–210.

50. Baciu, M., S. C. Sebai, …, A. Gee. 2006. Degradative transport of cationic amphiphilic drugs across phospholipid bilayers. *Philos. Trans. R. Soc. London A Math. Phys. Eng. Sci.* 364:2597–2614.

51. Swairjo, M. A., B. A. Seaton, and M. F. Roberts. 1994. Effect of vesicle composition and curvature on the dissociation of phosphatidic acid in small unilamellar vesicles a 31P-NMR study. *Biochim. Biophys. Acta.* 1191:354–361.

52. Madine, J., E. Hughes, …, D. A. Middleton. 2008. The effects of alpha-synuclein on phospholipid vesicle integrity: a study using 31P NMR and electron microscopy. *Mol. Membr. Biol.* 25:518–527.

53. Monette, M., M. R. Van Calsteren, and M. Lafleur. 1993. Effect of cholesterol on the polymorphism of dipalmitoylphosphatidylcholine/melittin complexes: an NMR study. *Biochim. Biophys. Acta.* 1149:319–328.

54. Gater, D. L., J. M. Seddon, and R. V. Law. 2008. Formation of the liquid-ordered phase in fully hydrated mixtures of cholesterol and lysopalmitoylphosphatidylcholine. *Soft Matter.* 4:263–267.

55. Baumgart, F., L. Loura, …, J. Pérez-Gil. 2009. Pulmonary surfactant protein C reduces the size of liquid ordered domains in a ternary membrane model system. *Biophys. J.* 96:608a–609a.

56. Nag, K., S. G. Taneva, …, K. M. Keough. 1997. Combinations of fluorescently labeled pulmonary surfactant proteins SP-B and SP-C in phospholipid films. *Biophys. J.* 72:2638–2650.

57. Wüstneck, R., J. Perez-Gil, …, U. Pison. 2005. Interfacial properties of pulmonary surfactant layers. *Adv. Colloid Interface Sci.* 117:33–58.

58. Bernardino de la Serna, J., G. Orädd, …, J. Perez-Gil. 2009. Segregated phases in pulmonary surfactant membranes do not show coexistence of lipid populations with differentiated dynamic properties. *Biophys. J.* 97:1381–1389.

59. Pérez-Gil, J., K. Nag, …, K. M. Keough. 1992. Pulmonary surfactant protein SP-C causes packing rearrangements of dipalmitoylphosphatidylcholine in spread monolayers. *Biophys. J.* 63:197–204.

60. Chavarha, M., R. W. Loney, …, S. B. Hall. 2015. Hydrophobic surfactant proteins strongly induce negative curvature. *Biophys. J.* 109: 95–105.

61. Chavarha, M., H. Khoojinian, …, S. B. Hall. 2010. Hydrophobic surfactant proteins induce a phosphatidylethanolamine to form cubic phases. *Biophys. J.* 98:1549–1557.

62. Chavarha, M., R. W. Loney, …, S. B. Hall. 2013. An anionic phospholipid enables the hydrophobic surfactant proteins to alter spontaneous curvature. *Biophys. J.* 104:594–603.

63. Poulain, F. R., L. Allen, …, S. Hawgood. 1992. Effects of surfactant apolipoproteins on liposome structure: implications for tubular myelin formation. *Am. J. Physiol.* 262:L730–L739.

64. Oosterlaken-Dijksterhuis, M. A., M. van Eijk, …, H. P. Haagsman. 1992. Lipid mixing is mediated by the hydrophobic surfactant protein SP-B but not by SP-C. *Biochim. Biophys. Acta.* 1110:45–50.

65. Plasencia, I., L. Rivas, …, J. Pérez-Gil. 2004. The N-terminal segment of pulmonary surfactant lipopeptide SP-C has intrinsic propensity to interact with and perturb phospholipid bilayers. *Biochem. J.* 377: 183–193.

66. Plasencia, I., K. M. W. Keough, and J. Perez-Gil. 2005. Interaction of the N-terminal segment of pulmonary surfactant protein SP-C with interfacial phospholipid films. *Biochim. Biophys. Acta.* 1713:118–128.

67. Gómez-Gil, L., J. Pérez-Gil, and E. Goormaghtigh. 2009. Cholesterol modulates the exposure and orientation of pulmonary surfactant protein SP-C in model surfactant membranes. *Biochim. Biophys. Acta.* 1788:1907–1915.

68. Orgeig, S., and C. B. Daniels. 2001. The roles of cholesterol in pulmonary surfactant: insights from comparative and evolutionary studies. *Comp. Biochem. Physiol. A Mol. Integr. Physiol.* 129:75–89.

69. Rinia, H. A., J. W. P. Boots, …, B. de Kruijff. 2002. Domain formation in phosphatidylcholine bilayers containing transmembrane peptides: specific effects of flanking residues. *Biochemistry.* 41:2814–2824.

70. Davis, J. H. 1979. Deuterium magnetic resonance study of the gel and liquid crystalline phases of dipalmitoyl phosphatidylcholine. *Biophys. J.* 27:339–358.

71. Sylvester, A., L. MacEachern, …, M. R. Morrow. 2013. Interaction of the C-terminal peptide of pulmonary surfactant protein B (SP-B) with a bicellar lipid mixture containing anionic lipid. *PLoS One.* 8:e72248.

Biophysical Journal, Volume *113*

Supplemental Information

Divide & Conquer: Surfactant Protein SP-C and Cholesterol Modulate Phase Segregation in Lung Surfactant

Nuria Roldan, Jesús Pérez-Gil, Michael R. Morrow, and Begoña García-Álvarez

Supplementary material

Divide and conquer: Phase segregation in Lung Surfactant is modulated by Surfactant Protein SP-C and Cholesterol

Nuria Roldan[1], Jesús Pérez-Gil[1], Michael R. Morrow[2], Begoña García-Álvarez[1]*

[1]Dept. of Biochemistry, Faculty of Biology, and Research Institute "Hospital 12 de Octubre", Complutense University, 28040 Madrid, Spain

[2]Dept. of Physics and Physical Oceanography, Memorial University of Newfoundland, St. John's, Newfoundland, Canada

*Corresponding Author

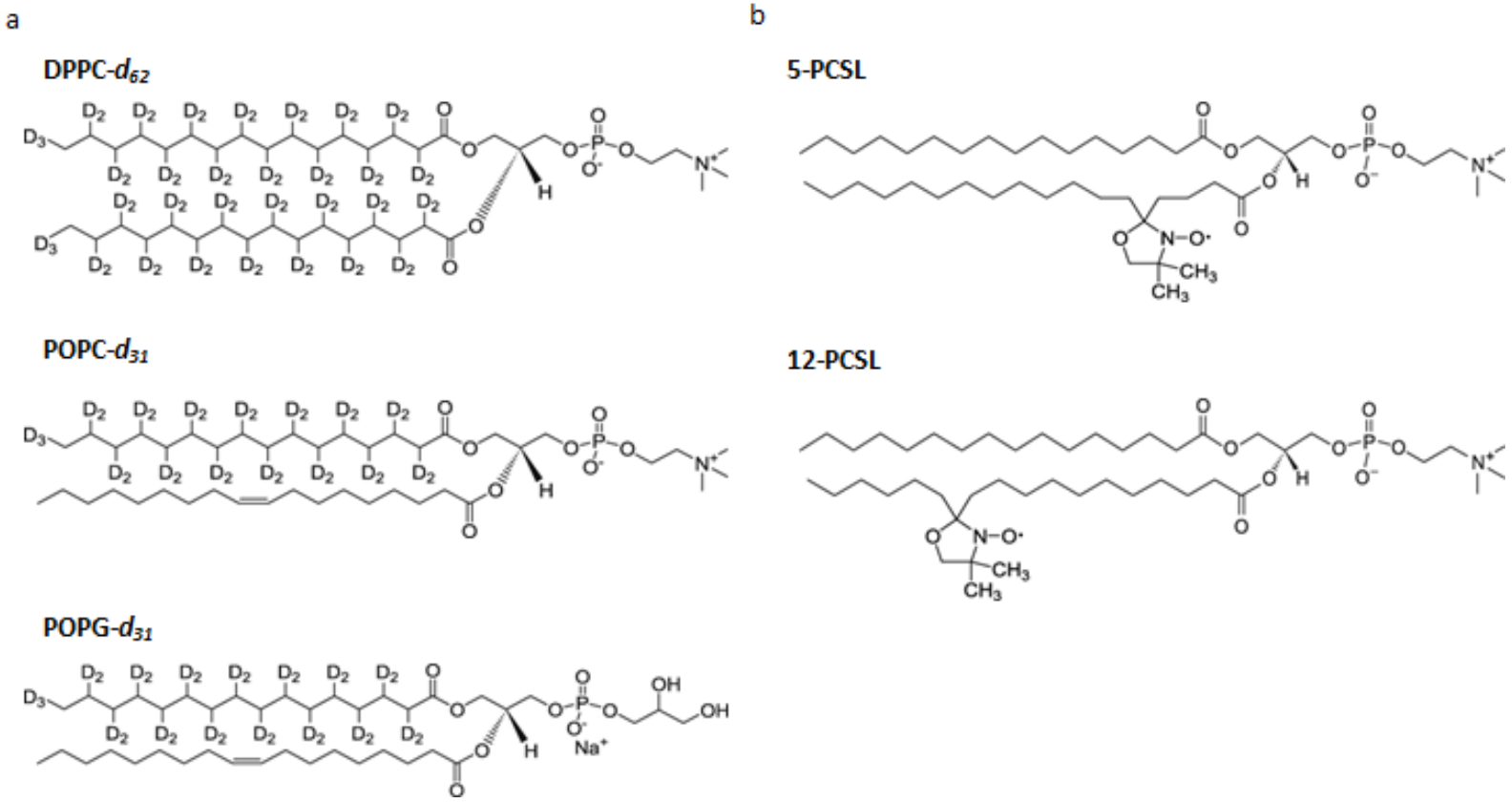

Supplementary Figure 1. a) Schematic representation of deuterium (D)-labelled lipids employed in this study. b) Scheme of the spin-labelled probes used for ESR experiments.

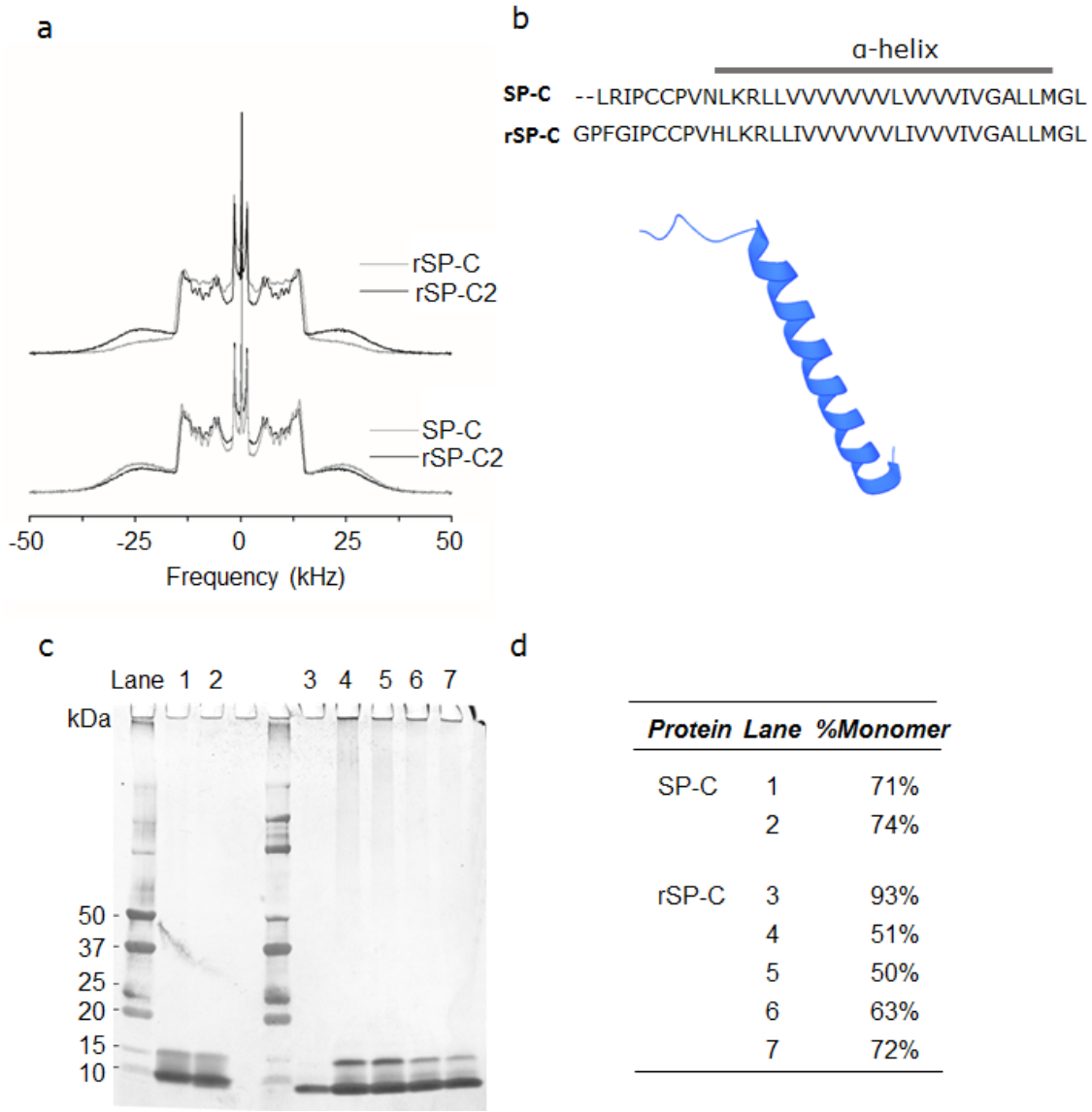

Protein	*Lane*	*%Monomer*
SP-C	1	71%
	2	74%
rSP-C	3	93%
	4	51%
	5	50%
	6	63%
	7	72%

Supplementary Figure 2. a) Powder spectra of DPPC-d_{62}/POPC/POPG at 37°C incorporating different protein stocks. Top spectra represent the difference between two rSP-C stocks, in particular the one presented in Fig. 1 (rSP-C, grey line), and a different one (rSP-C2, black line). Bottom spectra illustrate the similarities between the spectra containing native SP-C presented in Fig. 1 (SP-C, grey line) and the second stock of rSP-C tested (rSP-C2, black line). b) Amino acid sequence of native SP-C and the recombinant human form rSP-C with the helical stretch highlighted. The 3D structure of native SP-C is shown below (PDB 1SPF). c) Silver stained SDS electrophoresis gradient gel (4%-20% polyacrylamide) showing the running pattern of different SP-C and rSP-C batches. Lanes 1 and 2 correspond to two different SP-C stocks and 3-7, to five rSP-C batches. d) %monomer calculated for each protein form by a densitometry analysis.

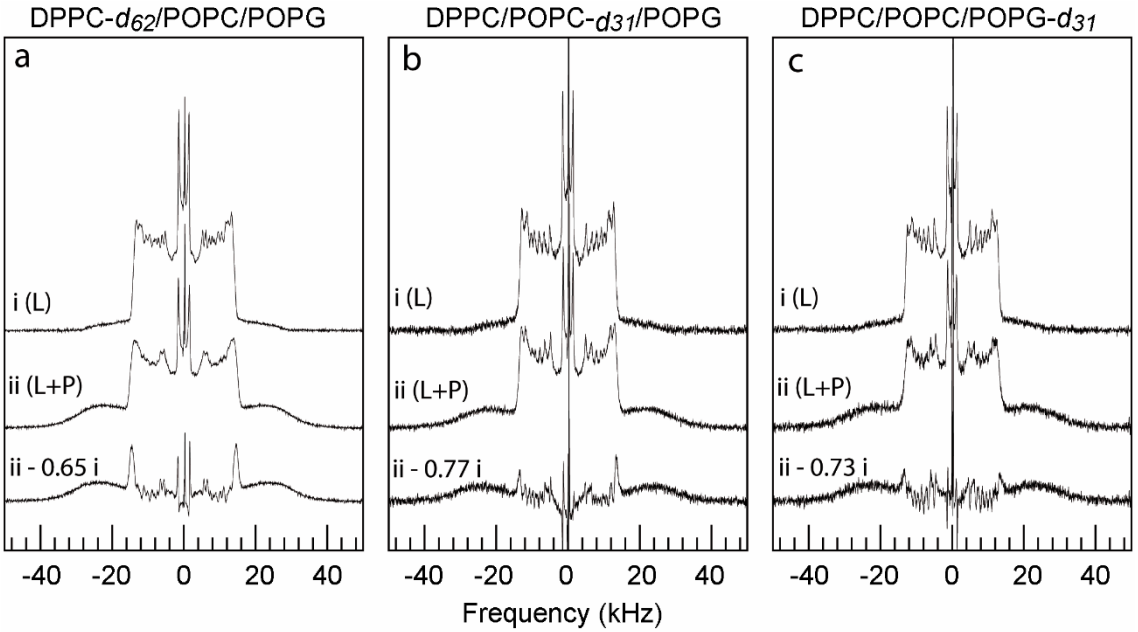

Supplementary Figure 3. Representation of the subtraction method employed to determine the amount of lipid forming part of the SP-C-induced ordered phase. The spectrum corresponding to lipid-only samples, i (L), was subtracted from that of protein-containing liposomes, ii (L+P) in a proportion (x) that eliminated the fluid region of the lipid-protein sample. Resulting spectra were obtained as: ii – x i. Some spectral components of the fluid phase remain in the subtracted spectrum since the fluid phase spectra with and without SP-C are not identical. Spectral subtractions are shown for the three lipid systems studied: DPPC-d_{62}/POPC/POPG (a), DPPC/POPC-d_{31}/POPG (b) and DPPC/POPC/POPG-d_{31} (c).

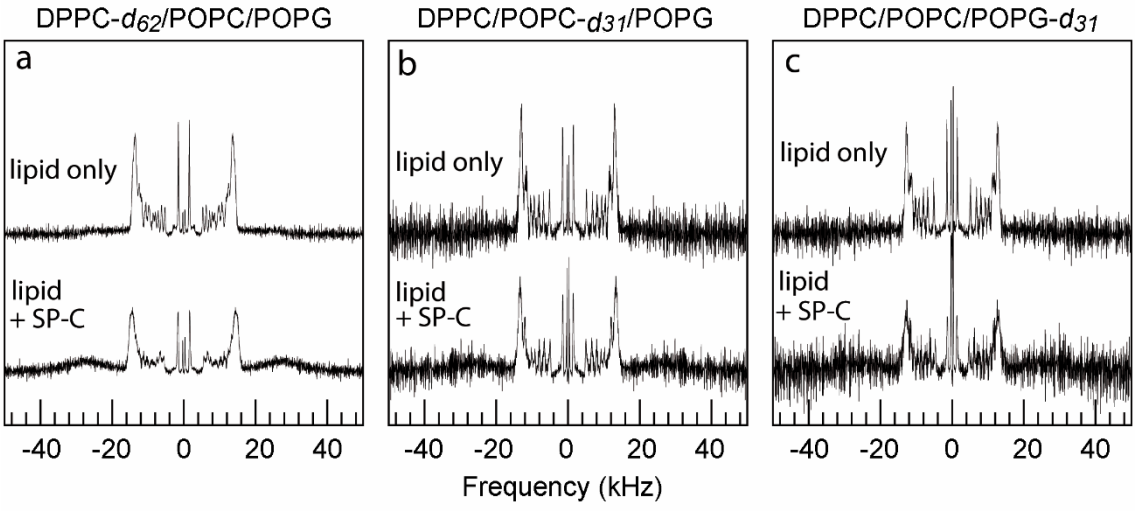

Supplementary Figure 4. DePaked spectra for the liquid crystalline phase of each spectrum in the presence and absence of SP-C and no cholesterol. Almost no differences in the splitting distributions are observable between the lipid only and SP-C-associated spectrum. DePaking is shown for the three lipid systems studied: DPPC-d_{62}/POPC/POPG (a), DPPC/POPC-d_{31}/POPG (b) and DPPC/POPC/POPG-d_{31} (c).

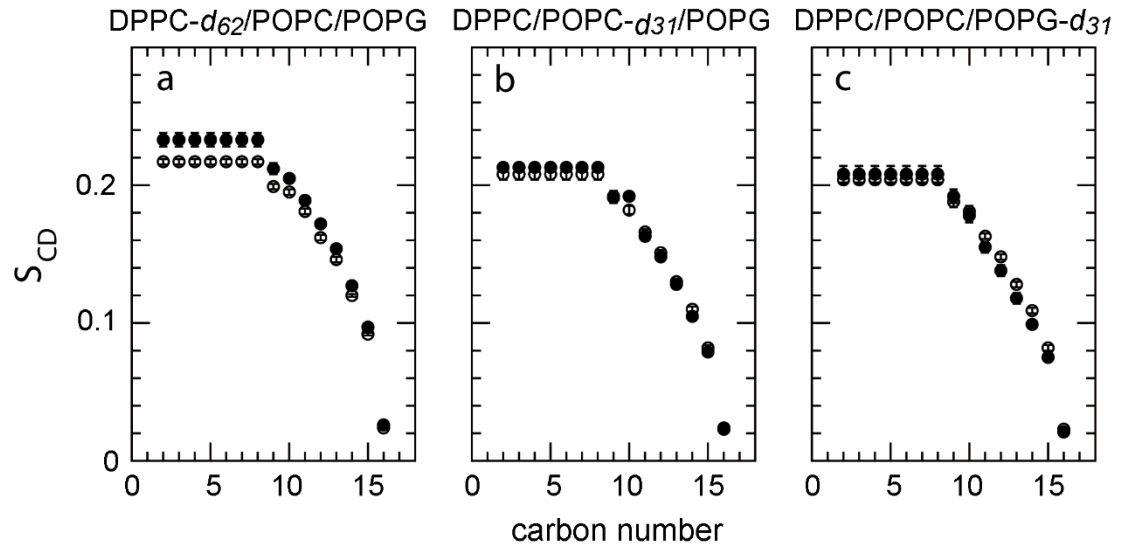

Supplementary Figure 5. Order parameter plots obtained from the dePaked spectra shown in Supplementary Figure 4. Filled symbols represent SP-C-containing liposomes and empty symbols correspond to lipid-only vesicles. The assignments for DPPC doublets were performed as described elsewhere (72). POPC and POPG doublets were assigned using the protocol in (73). The three lipid systems studied are represented: DPPC-d_{62}/POPC/POPG (a), DPPC/POPC-d_{31}/POPG (b) and DPPC/POPC/POPG-d_{31} (c).

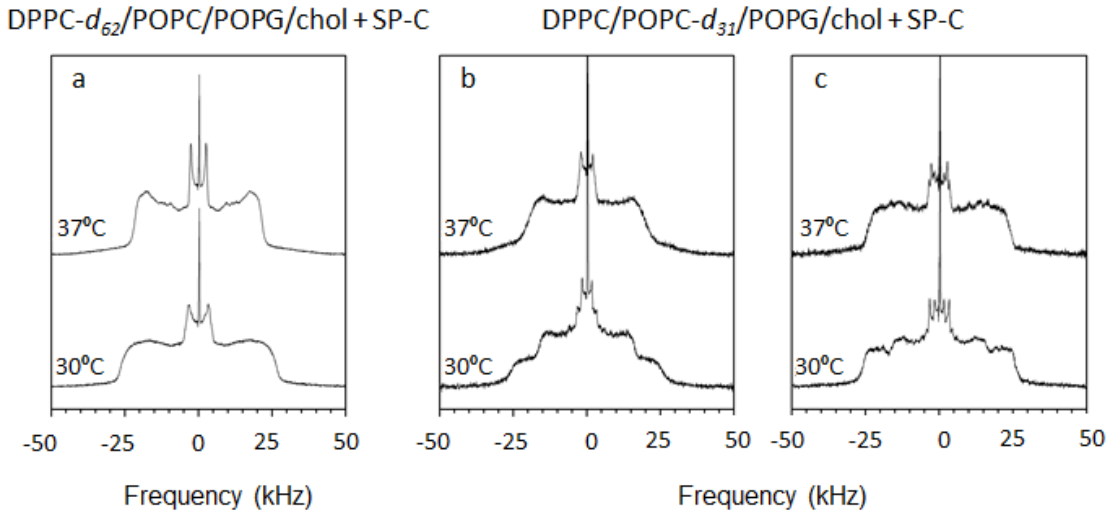

Supplementary Figure 6. (a) Powder ^{2}H NMR spectra of DPPC-d_{62}/POPC/POPG incorporating 10 wt% cholesterol and 5 wt% (1 mol%) SP-C at 30^{o}C. The spectra show lipid reorientations too slow to be axially symmetric on the experiment timescale. No phase separation is observed. (b,c) ^{2}H NMR spectra of multilamellar vesicles made of DPPC/POPC-d_{31}/POPG + 10 wt% Cholesterol and 5 wt% (1 mol%) SP-C. Each panel represents an independent experiment performed with a newly prepared sample incorporating different stocks of SP-C. Spectra at 30^{o}C are characteristic of a two-component phase segregation that is not apparent in the corresponding spectra at 37^{o}C. Differences found between replicates are likely due to slight different cholesterol concentrations found between the lipid stocks used to prepare these samples.

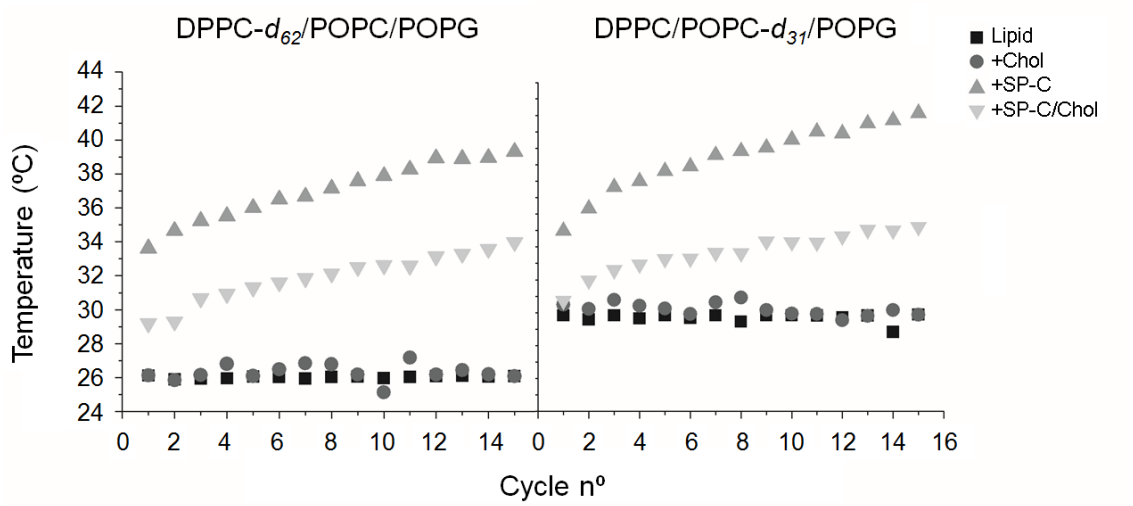

Supplementary Figure 7. Melting temperature of DPPC-d_{62} and POPC-d_{31}-containing systems as determined from DSC thermograms. Calculated T_m is represented with respect to each heating cycle from 15 to 60°C. As observed, for the lipid alone systems, the melting temperature changed by 4°C depending on the incorporation of DPPC-d_{62} or POPC-d_{31}. No effect of cholesterol was observed. The incorporation of SP-C raised the melting temperature abruptly reducing the gap between the two lipid systems and increasing the differences between SP-C and SP-C/Chol-containing liposomes. Over the number of cycles tested, the observed transition temperature for samples containing protein continued to increase with each cycle.

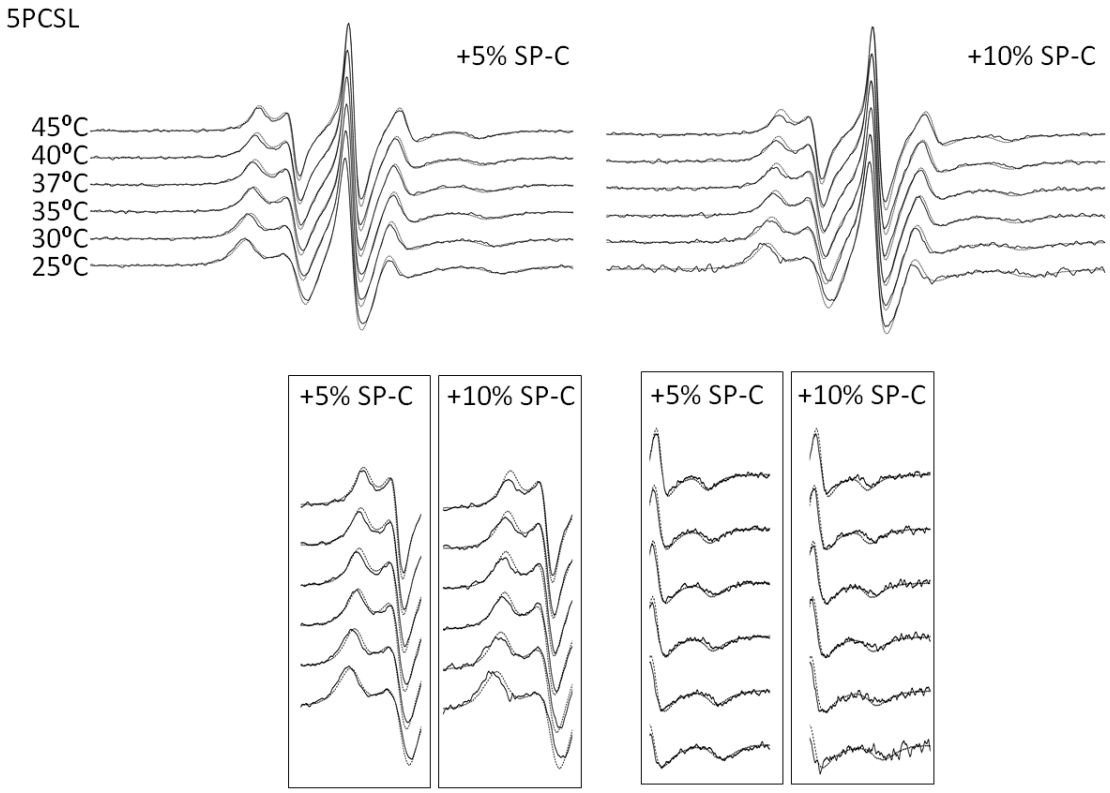

Supplementary Figure 8. ESR spectra of DPPC/POPC/POPG vesicles incorporating no protein (dotted line), 5 wt% (1 mol%) or 10 wt% (2 mol%) SP-C (solid lines) labelled with 1 mol% of the probe 5PSCL at different temperatures. Spectra below correspond to magnifications showing a detailed view of the low and high-field spectra for vesicles with no protein (dotted line), and samples containing either 5 wt% (1 mol%) SP-C or 10 wt% (2 mol%) SP-C (solid lines). The total scan range was 100G.